Group II metal complexes with the *N*-(2-oxy-3,5-di-*tert*-butylphenyl)-4,6-di-*tert*-butyl-*o*-iminobenzoquinone ligand: an ESR study*

A. V. Piskunov, O. Yu. Trofimova, S. Yu. Ketkov, G. K. Fukin, V. K. Cherkasov, and G. A. Abakumov*

G. A. Razuvaev Institute of Organometallic Chemistry, Russian Academy of Sciences, 49 ul. Tropinina, 603950 Nizhnii Novgorod, Russian Federation. Fax: +7 (831) 462 7497. E-mail: pial@iomc.ras.ru

The Group II metal (Mg, Ca, Sr, Ba, Zn, Cd) complexes based on the paramagnetic *N*-(2-oxy-3,5-di-*tert*-butylphenyl)-4,6-di-*tert*-butyl-*o*-iminobenzoquinone ligand were generated in solutions and studied by ESR spectroscopy. The magnesium, zinc, and cadmium complexes with trialkylphosphine ligands were prepared. Their molecular structures and electron density distribution were studied by ESR spectroscopy and DFT calculations.

Key words: paramagnetic organic ligand, Group II metals, trialkylphosphines, ESR spectroscopy.

Metal complexes based on the tridentate redox-active *N*-(2-oxy-3,5-di-*tert*-butylphenyl)-4,6-di-*tert*-butyl-*o*-iminobenzoquinone ligand attract great attention since the first compounds of such type have been obtained.[1—3] These complexes were first synthesized upon oxidation of 3,5-di-*tert*-butyl-*o*-aminophenol with atmospheric oxygen in the presence of Group IV element (Ge, Sn, Pb) organohalides. More recently, a template reaction of ammonia and 3,5-di-*tert*-butylpyrocatechol involving metal salts and atmospheric oxygen was proposed to obtain such compounds.[4] This reaction allows preparation of compounds containing the *N*-(2-oxy-3,5-di-*tert*-butylphenyl)-4,6-di-*tert*-butyl-*o*-iminobenzoquinone ligand with various metals.[5—14] This ligand can exist in the metal coordination sphere in four different redox states (Scheme 1).

The neutral (L^0) and dianionic (L^2) ligand forms are paramagnetic, while the monoanionic (L^1) and trianionic (L^3) forms are diamagnetic. It should be noted that the template reaction discovered in 1975 allows no control of the redox state of the organic ligand in the metal complexes that formed. Generally, two-, three-, and four-valence metals form compounds of the type $M^{II}L^1_2$, $L^1M^{III}L^2$, and $M^{IV}L^2_2$, respectively.[5—9,11—14] The syntheses based on the rare-earth element salts afford the nine-coordinate derivatives $M^{III}L^1_3$ (see Ref. 10). Only one paramagnetic Group II metal complex containing the dianion L^2,

Scheme 1

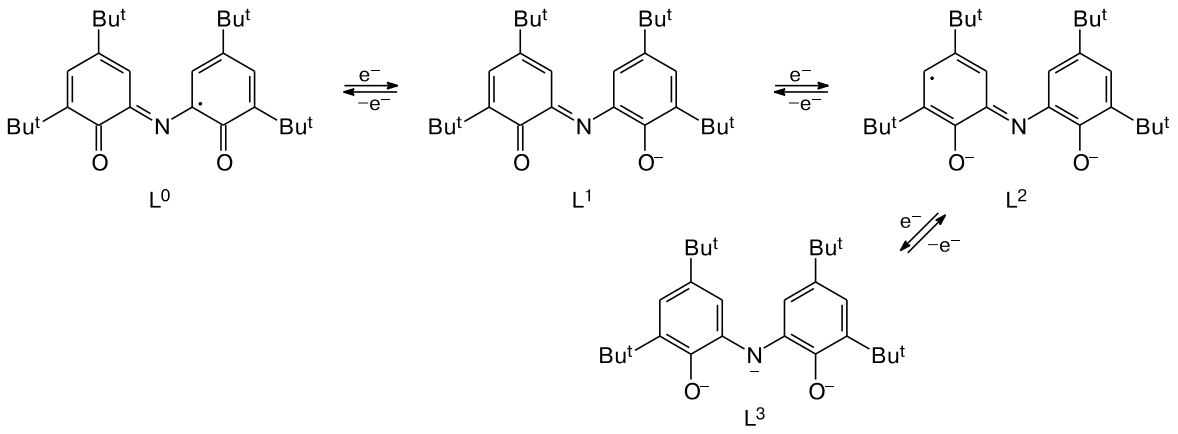

* Dedicated to the Academician of the Russian Academy of Sciences R. Z. Sagdeev on the occasion of his 70th birthday.

Published in Russian in *Izvestiya Akademii Nauk. Seriya Khimicheskaya,* No. 12, pp. 2473—2481, December, 2011.

viz., $ZnL^2 \cdot Et_3N$, have been described[15] up to date. The formula L^0ZnL^2 was first attributed[15] to another metastable zinc complex with the paramagnetic *N*-(2-oxy-3,5-di-*tert*-butylphenyl)-4,6-di-*tert*-butyl-*o*-iminobenzoquinone. However, recent theoretical studies[16] suggest that this compound should be considered as the complex ZnL^1_2 where one of the L^1 ligands is in the excited triplet state.

In the present work, we reported the generation and ESR study of the Group II metal (Mg, Ca, Sr, Ba, Zn, Cd) complexes with the *N*-(2-oxy-3,5-di-*tert*-butylphenyl)-4,6-di-*tert*-butyl-*o*-iminobenzoquinone ligand in solution.

Results and Discussion

Paramagnetic compounds **2a**—**f** were prepared by reduction of the six-coordinate complexes **1a**—**f** in two different manners (Scheme 2).

Scheme 2

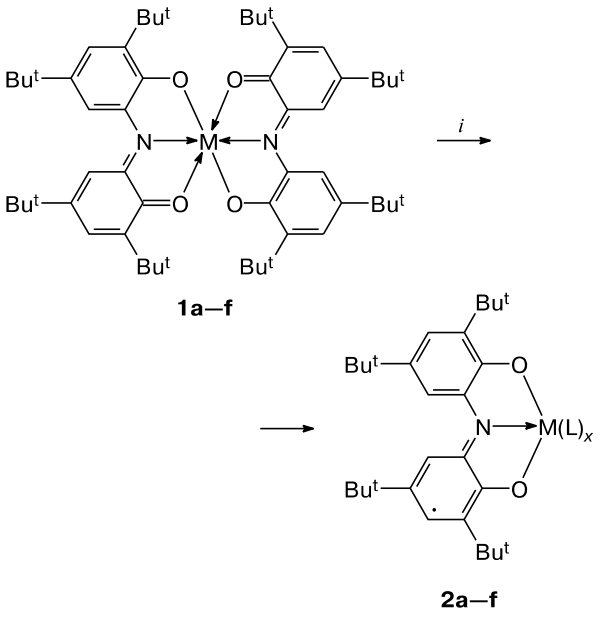

i. $DAD^{-1}MI$ (0.5 equiv.), THF (for **2a,b,e**); Sr, THF (for **2c**); Ba, $MeOCH_2CH_2OMe$ (DME) (for **2d**); Cd, pyridin (for **2f**).

DAD is 1,4-xylyldiazabuta-1,3-diene.
M = Mg (**a**), Ca (**b**), Sr (**c**), Ba (**d**), Zn (**e**), Cd (**f**)
L = THF (**2a**—**c**,**e**), DME (**2d**), Py (**2f**)

The strontium (**2c**), barium (**2d**), and cadmium (**2f**) derivatives form in the reaction of complexes **1c**,**d**,**f** with the corresponding metalls in THF, 1,2-dimethoxyethane (DME), and pyridine, respectively. Reduction of complexes **1a**,**b**,**e** with metals, such as magnesium, calcium, and zinc, proceeds slowly and, therefore, the radical ion derivatives $DAD^{-1}MI$ (M = Mg, Ca, Zn, DAD is 1,4-xylyldiazabuta-1,3-diene) were used as reducing agents for the preparation of compounds **2a**,**b**,**e**. Such derivatives can be readily prepared by the reaction of metals with DAD in the presence of I_2 or the corresponding metal iodides.[17—19]

The solutions of compounds **2a**—**f** demonstrate well-defined isotropic ESR spectra (Fig. 1). Their hyperfine structures (HFS) are caused by hyperfine interaction (HFI) of the unpaired electron with two pairs of equivalent protons ^1H (99.98%, $I = 1/2$, $\mu_N = 2.7928$)[20] and one ^{14}N nuclei (99.63%, $I = 1$, $\mu_N = 0.4037$).[20] The spectra of compounds **2d** and **2f** display additional satellite splitting induced by HFI of the unpaired electron with the magnetic isotopes ^{135}Ba (6.59%, $I = 3/2$, $\mu_N = 0.8365$), ^{137}Ba (11.23%, $I = 3/2$, $\mu_N = 0.9357$),[20] and ^{111}Cd (12.81%, $I = 1/2$, $\mu_N = -0.5943$), ^{113}Cd (12.22%, $I = 1/2$, $\mu_N = -0.6217$),[20] respectively. The ESR spectral parameteres of compounds **2a**—**f** are given in Table 1. The presence of HFI with two pairs of equivalent protons in the ESR spectra of compounds **2a**—**f** suggets that the unpaired electron is delocalized between the rings of the paramagnetic tridentate ligand. This fact and the values of HFI constants with the magnetic nuclei of the organic ligand are in good agreement with the results of the ESR studies of germanium,[1] tin,[2,21,22] and lead complexes[3,22] based on the paramagnetic anion L^2. It should be noted that the data obtained in the present work are inconsistent with the ESR spectral data for the complex $ZnL^2 \cdot Et_3N$ (see Ref. 15), for which an asymmetric spin density distribution in the paramagnetic ligand was proposed. However, the interpretation of the ESR spectrum of complex $ZnL^2 \cdot Et_3N$ observed in Ref. 15 is doubtful. First, great linewidths in the spectrum do not allow one to make unambiguous line assignment. Second, the triethylamine ligand being in the plane of the paramagnetic ligand cannot provide a high value of the HFI constant (0.19 mT) with the ^{14}N magnetic nucleus (this value is typically no greater than 0.1 mT for the metal complexes with the paramagnetic ligands containing coordinated amines (see Refs 23 and 24)). In addition, the number of lines, the line intensity ratios, and the extension of the ESR spectrum observed in Ref. 15 are very close to the recently described[22] spectrum of the radical cation of the protonated neutral (O,N,O) ligand form $[L^0H]^+$. To check the results obtained, we performed additional experiments. Complex **2e** was prepared from compound **1e** enriched (87.5 %) with the ^{67}Zn isotope (natural abundance is 4.1%, $I = 5/2$, $\mu_N = 0.8752$). Except for the satellite line width, the ESR spectrum obtained (see Fig. 1, *c*) repeats the observed spectrum of complex **2e** with the natural zinc isotope distribution and is well simulated (see Fig. 1, *d*) taking into account the abundance of the magnetic ^{67}Zn isotope (43.75%). Such amount of the ^{67}Zn isotope is caused by the preparation method of **2e** (see Scheme 2), which results in twofold dilution of ^{67}Zn in the complex that formed.

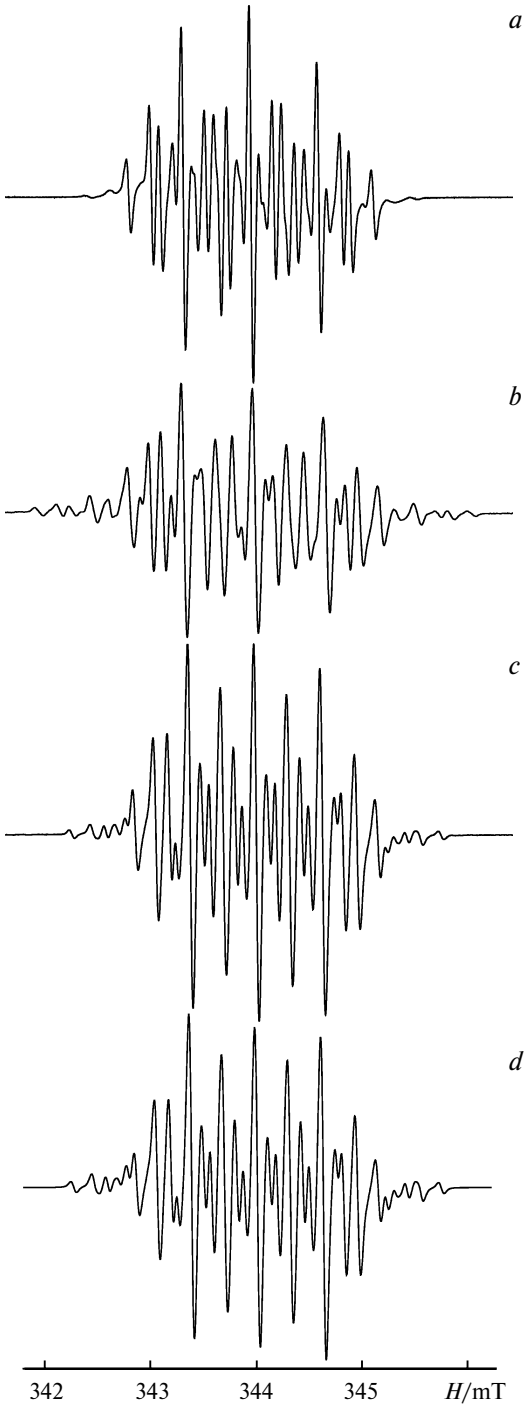

Fig. 1. Experimental isotropic ESR spectra of complex **2d** in DME (*a*) and complex **2f** in Py (*b*), as well as the experimental spectrum of complex **2e** ([^{67}Zn] = 43.75%) in THF (*c*) and its simulation (*d*). T = 290 K.

We found that the paramagnetic complexes **2a**—**f** are unstable in solution. Keeping solutions of **2a**—**f** under the conditions excluding the oxygen and air moisture access is accompanied by sedimentation of a white precipitate and by a decrease in the signal intensity in the ESR spectrum. Replacement of the solvent by evaporation of THF under reduced pressure followed by dissolution of the residue in diethyl ether or toluene results in solutions of the compounds having no signals in the ESR spectrum. Long-term keeping a solution of compound **2d** in dimethoxyethane at room temperature leads to crystallization of a dark-green diamagnetic complex **3**, which is likely the comproportionation product (Scheme 3).

Scheme 3

$$4\ BaL^2 \cdot DME_x \rightleftharpoons BaL^1{}_2 \cdot DME_2 + Ba_3L^3{}_2 \cdot DME_y$$

2d **3**

The molecular structure of complex **3** was established by X-ray analysis (Fig. 2). The unit cell of complex **3** contains two independent molecules. Since the bond angles and bond lengths in them differ slightly, the molecular structure of **3** is discussed by the example of one molecule. Selected bond lengths and bond angles for complex **3** are given in Table 2. The barium atom in complex **3** is decacoordinated. The metal coordination sphere is formed by two (O,N,O) ligands and two dimethoxyethane molecules. The tridentate ligands are in *trans*-position to each other. The dihedral angle between the O(1)—N(1)—O(2) and O(3)—N(2)—O(4) planes is 42.09°. A comparison of geometric parameters (C—C, C—O, and C—N bond lengths) of the (O,N,O) ligands with the published data[11,13,15] evidences their monoanionic nature. The redox-active ligands are nonplanar, *i.e.*, the dihedral angles between the planes C(1)—C(6) and O(1)—N(1)—O(2), C(15)—C(20) and O(1)—N(1)—O(2), C(29)—C(34) and O(3)—N(2)—O(4), C(43)—C(48) and O(3)—N(2)—O(4) are 28.75°, 19.93°, 22.03°, and 19.29°, respectively.

The ESR spectra do not allow one to determine the number and arrangement of neutral donor ligands completing the metal coordination sphere in the paramag-

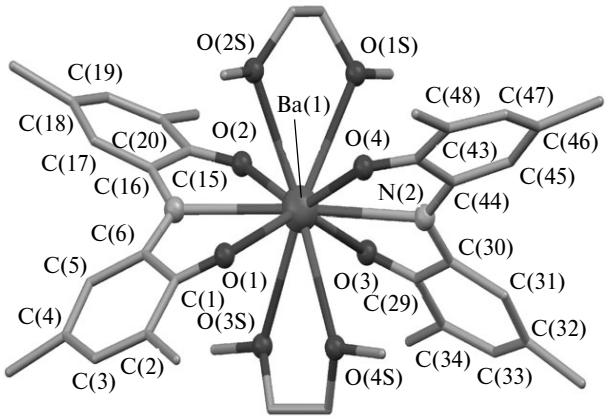

Fig. 2. Molecular structure of complex **3**. The hydrogen atoms and methyl groups of *tert*-butyl substituents are not shown.

Table 1. Parameters of the experimental and DFT-calculated[a] ESR spectra of complexes **2a—f**, **4** and **5a—c**

Complex	g_i	$a_i(2H)$	$a_i(2H)$	$a_i(^{14}N)$	$a_i(M)$[b]	$a_i(^{31}P)$
				mT		
2a	2.0036	0.212	0.325	0.607	—	—
2b	2.0036	0.216	0.312	0.619	—	—
2c	2.0033	0.215	0.306	0.603	—	—
2d	2.0029	0.217	0.301	0.642	0.241 [^{135}Ba] 0.270 [^{137}Ba]	—
2e	2.0026	0.196	0.326	0.629	0.249 [^{67}Zn]	—
2f	2.0021	0.197	0.302	0.673	1.577 [^{111}Cd] 1.650 [^{113}Cd]	—
4	2.0034	0.213 (0.240)	0.327 (0.386)	0.606 (0.586)	—	—
5a[c]	2.0029	0.180 (0.212)	0.293 (0.326)	0.638 (0.634)	0.320 (0.280) [^{67}Zn]	1.727 (1.658)
5b[c]	2.0020	0.184 (0.225)	0.304 (0.350)	0.677 (0.860)	1.759 (1.860) [^{111}Cd] 1.840 (1.945) [^{113}Cd]	0.977 (0.750)
5c[d]	2.0029	0.175	0.295	0.654	0.320 [^{67}Zn]	2.263 0.661

[a] Given in parentheses.
[b] The isotope to which the ESR spectral line is related is shown in square brackets.
[c] The $a_i(^{31}P)$ value is given for both ^{31}P atoms in the structures of **5a,b**.
[d] The $a_i(^{31}P)$ value is given for each ^{31}P atom in the structure of **5c**.

netic complexes **2a—f**. It is known[25,26] that various phosphines are promising ligands allowing one to study the composition and structure of the metal coordination sphere in solution by ESR spectroscopy. However, no ESR spectra of the Group II metal complexes containing phosphines and paramagnetic organic ligands have been recorded earlier. In the present work, we established that the radical complexes of magnesium, zinc, and cadmium (**2a**,**e**,**f**) can coordinate trimethylphosphine in THF (Scheme 4). The addition of excess phosphine shifts the equilibrium toward the formation of paramagnetic derivatives (see Scheme 3). For instance, the addition of

Table 2. Selected bond lengths and angles in complex **3**

Bond	d/Å	Angle	ω/deg	Bond	d/Å	Angle	ω/deg
Ba(1)—O(3)	2.752(2)	O(3)—Ba(1)—O(2)	75.06(5)	C(5)—C(6)	1.365(3)	O(4)—Ba(1)—N(2)	56.56(5)
Ba(1)—O(2)	2.767(2)	O(3)—Ba(1)—O(4)	112.89(5)	C(15)—C(20)	1.458(3)	O(1)—Ba(1)—N(2)	125.61(5)
Ba(1)—O(4)	2.773(2)	O(2)—Ba(1)—O(4)	146.21(5)	C(15)—C(16)	1.477(3)	O(2S)—Ba(1)—N(2)	114.32(5)
Ba(1)—O(1)	2.812(2)	O(3)—Ba(1)—O(1)	144.85(5)	C(16)—C(17)	1.427(3)	O(3S)—Ba(1)—N(2)	105.76(6)
Ba(1)—N(2)	2.920(2)	O(2)—Ba(1)—O(1)	111.54(5)	C(17)—C(18)	1.354(3)	O(4S)—Ba(1)—N(2)	69.98(6)
Ba(1)—N(1)	2.943(2)	O(4)—Ba(1)—O(1)	81.38(5)	C(18)—C(19)	1.435(3)	O(3)—Ba(1)—O(1S)	78.38(5)
Ba(1)—O(1S)	2.934(2)	O(3)—Ba(1)—O(2S)	131.95(5)	C(19)—C(20)	1.359(3)	O(2)—Ba(1)—O(1S)	75.37(5)
Ba(1)—O(2S)	2.884(2)	O(2)—Ba(1)—O(2S)	75.59(5)	C(29)—C(34)	1.455(4)	O(4)—Ba(1)—O(1S)	74.45(5)
Ba(1)—O(3S)	2.903(2)	O(4)—Ba(1)—O(2S)	75.69(5)	C(29)—C(30)	1.463(4)	O(1)—Ba(1)—O(1S)	136.65(5)
Ba(1)—O(4S)	2.915(2)	O(1)—Ba(1)—O(2S)	81.78(5)	C(30)—C(31)	1.427(3)	O(2S)—Ba(1)—O(1S)	57.81(5)
N(1)—C(2)	1.349(3)	O(3)—Ba(1)—O(3S)	68.23(5)	C(31)—C(32)	1.342(4)	O(3S)—Ba(1)—O(1S)	142.10(5)
N(1)—C(16)	1.349(3)	O(2)—Ba(1)—O(3S)	79.03(5)	C(32)—C(33)	1.445(4)	O(4S)—Ba(1)—O(1S)	136.85(5)
N(2)—C(44)	1.335(3)	O(4)—Ba(1)—O(3S)	134.75(5)	C(33)—C(34)	1.361(4)	N(2)—Ba(1)—O(1S)	67.19(5)
N(2)—C(30)	1.352(3)	O(1)—Ba(1)—O(3S)	78.97(5)	C(43)—C(48)	1.457(3)	O(3)—Ba(1)—N(1)	120.35(5)
O(1)—C(1)	1.258(3)	O(2S)—Ba(1)—O(3S)	139.61(5)	C(43)—C(44)	1.471(3)	O(2)—Ba(1)—N(1)	56.32(5)
O(2)—C(15)	1.253(3)	O(3)—Ba(1)—O(4S)	82.52(6)	C(44)—C(45)	1.420(3)	O(4)—Ba(1)—N(1)	126.76(5)
O(3)—C(29)	1.265(3)	O(2)—Ba(1)—O(4S)	135.42(6)	C(45)—C(46)	1.351(4)	O(1)—Ba(1)—N(1)	55.22(5)
O(4)—C(43)	1.263(3)	O(4)—Ba(1)—O(4S)	78.11(6)	C(46)—C(47)	1.434(4)	O(2S)—Ba(1)—N(1)	69.50(5)
C(1)—C(2)	1.461(3)	O(1)—Ba(1)—O(4S)	68.76(5)	C(47)—C(48)	1.372(3)	O(3S)—Ba(1)—N(1)	70.32(5)
C(1)—C(6)	1.462(3)	O(2S)—Ba(1)—O(4S)	142.99(5)			O(4S)—Ba(1)—N(1)	107.86(5)
C(2)—C(3)	1.428(3)	O(3S)—Ba(1)—O(4S)	56.82(5)			N(2)—Ba(1)—N(1)	175.98(6)
C(3)—C(4)	1.365(3)	O(3)—Ba(1)—N(2)	56.39(5)			O(1S)—Ba(1)—N(1)	115.21(5)
C(4)—C(5)	1.432(3)	O(2)—Ba(1)—N(2)	122.65(5)				

Scheme 4

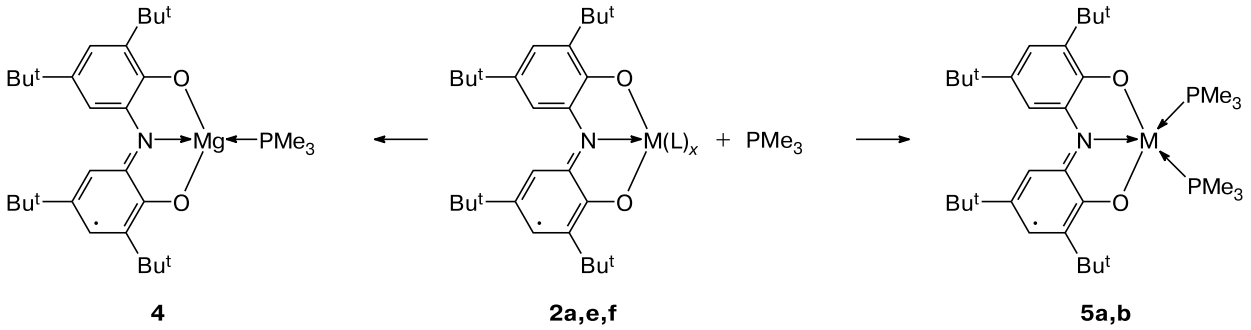

2: M = Mg (**a**), Zn (**e**), Cd (**f**); **5**: M = Zn (**a**), Cd (**b**)

Me_3P to a solution of the magnesium derivative **2a** results in a twentyfold increase in the signal intensity in the ESR spectrum. But we failed to reveal an additional HFS caused by HFI of the unpaired electron with the magnetic ^{31}P nucleus of the phosphine ligand in the observed ESR spectrum of complex **4**. This is likely due to the planar structure of complex **4** where the phosphine ligand being coordinated is near the plane of the paramagnetic ligand. This configuration of the copper(I) phosphine *o*-semiquinone complexes is characterized[25,27] by small values of the HFI constants with the ^{31}P nucleus (from 0 to 0.1 mT).

In contrast to the magnesium derivatives, the zinc and cadmium derivatives coordinate two trimethylphoshpine molecules (see Scheme 4), which is demonstrated by the ESR spectra of the complexes **5a** (Fig. 3) and **5b** (Fig. 4). Their HFS are caused by additional HFI with two equivalent phosphorus nuclei (see Table 1). The introduction of phosphine ligands into the zinc and cadmium complexes results in a spin density redistribution in the radical derivatives, which is manifested in a slight decrease in the HFI constants with the magnetic nuclei of the paramagnetic ligand and an increase in the HFI constants with the magnetic isotopes of metals on going from **2e**,**f** to **5a**,**b**. The values of the HFI constants with the ^{31}P nuclei in **5a** are close to those observed[25] for tetrahedral copper(I) bisphosphine *o*-semiquinone complexes; however, the values for the cadmium derivative **5b** are almost halved (which is likely caused by the increase in the metal—phosphorus

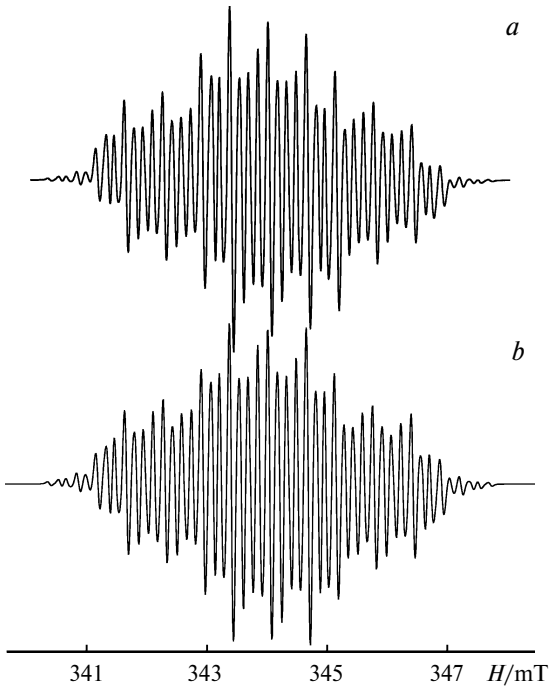

Fig. 3. Experimental isotropic ESR spectrum of complex **5a** ([^{67}Zn] = 43.75%) in THF (*a*) and its simulation (*b*). T = 290 K.

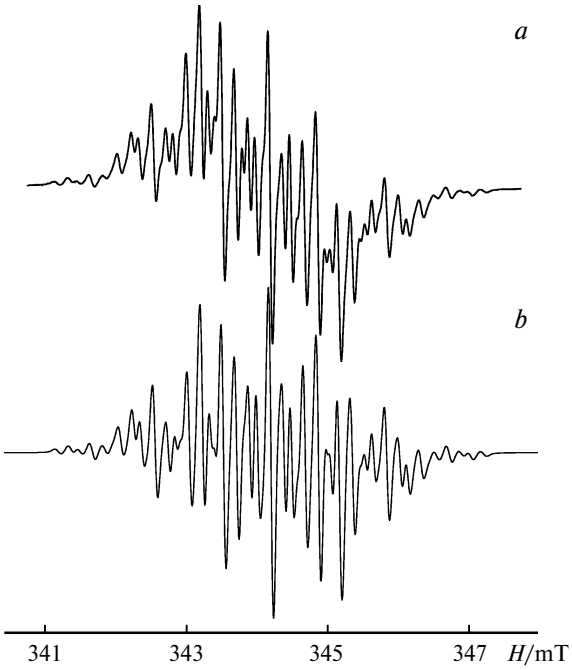

Fig. 4. Experimental isotropic ESR spectrum of complex **5b** in THF (*a*) and its simulation (*b*). T = 290 K.

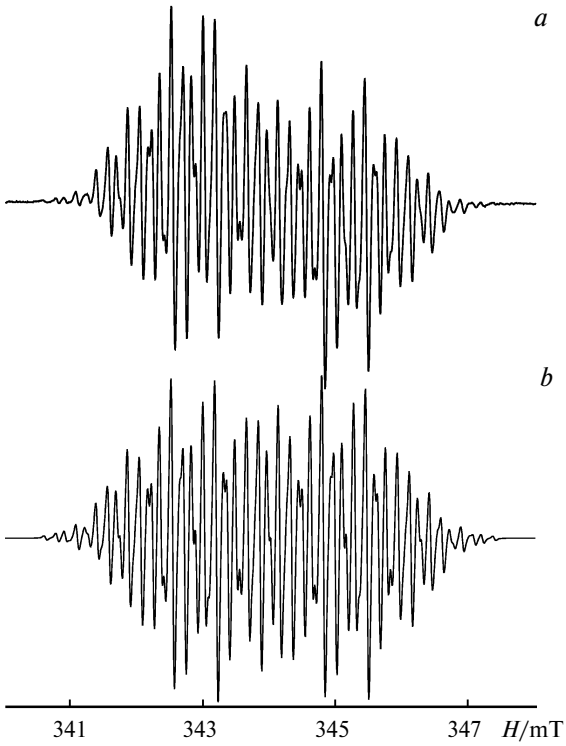

Fig. 5. Experimental isotropic ESR spectrum of complex **5c** ([^{67}Zn] = 43.75%) in THF (*a*) and its simulation (*b*). $T = 290$ K.

distance on going from zinc to cadmium). This is confirmed by comparison of the bond lengths in the isostructural zinc[28] and cadmium[29] bis-phoshpine complexes. The addition of tris-*tert*-butylphosphine to a solution of complex **5a** results in the appearance of a new ESR spectrum (Fig. 5, see Table 1), which displays HFI with two nonequivalent phosphorus atoms. This is explained by replacement of one trimethylphosphine ligand with a more electron-donating tris-*tert*-butylphosphine to form complex **5c** (Scheme 5).

Due to a great steric nonequivalence in complex **5c**, a more bulky PBu^t_3 ligand should be closer to the plane of the (O,N,O) radical ligand while trimethylphosphine should be closer to the apical position. As a consequence, in the ESR spectrum of complex **5c** the HFI constant with the phoshporus atom of the PBu^t_3 ligand is 0.66 mT and that with the phoshporus atom of the PMe_3 group increases to 2.26 mT as compared with complex **5a**.

We performed DFT calculations of the phoshpine complexes **4**, **5a**,**b** in the doublet state. The optimized structures of the complexes are shown in Fig. 6. Selected bond lengths and angles are given in Table 3. The calculated HFI constants with the magnetic nuclei, for which significant values are observed in the experimental spectrum, are given in Table 1. In general, the calculated values of the HFI constants are in good agreement with the experimental data, which indicates a correct choice of the computational method used. Despite the fact that the molecu-

Scheme 5

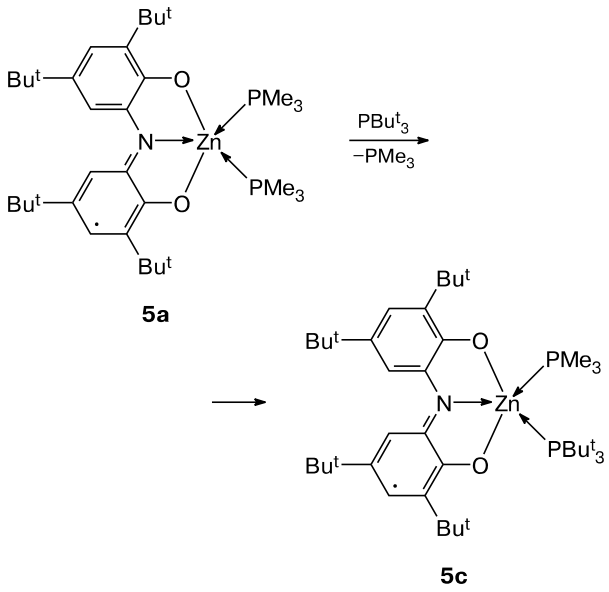

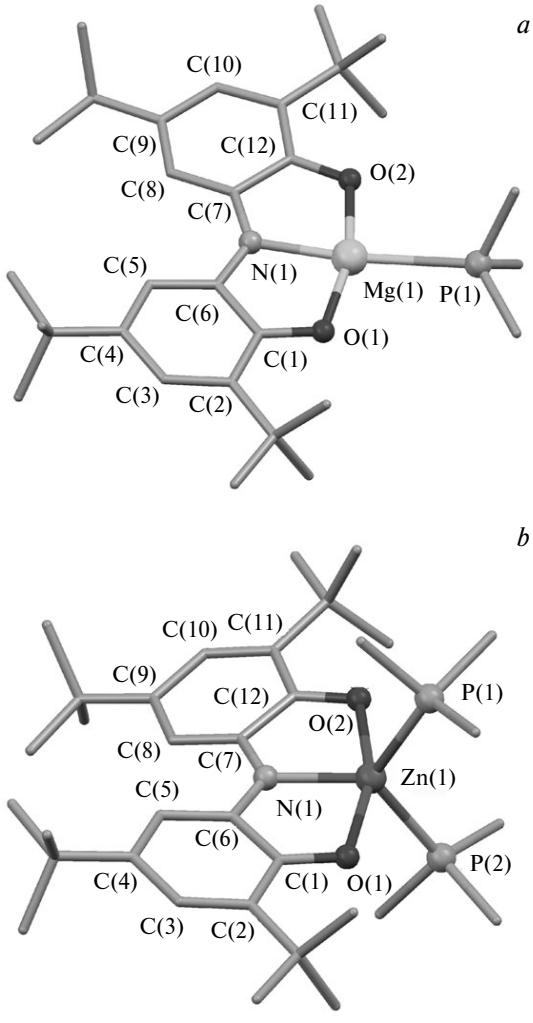

Fig. 6. Optimized structures of complexes **4** (*a*) and **5a** (*b*).

Table 3. Selected bond lengths and angles in complexes **4** and **5a,b** according to DFT calculations

Bond	*d*/Å			Angle	ω/deg		
	4	**5a**	**5b**		**4**	**5a**	**5b**
C(1)—O(1)	1.321	1.309	1.314	O(1)—M(1)—N(1)	82.01	80.40	72.97
C(1)—C(2)	1.427	1.433	1.437	O(2)—M(1)—N(1)	81.82	80.40	72.97
C(2)—C(3)	1.392	1.391	1.393	O(1)—M(1)—O(2)	163.81	160.81	145.93
C(3)—C(4)	1.418	1.417	1.419	P(1)—M(1)—N(1)	174.33	120.37	116.83
C(4)—C(5)	1.384	1.385	1.386	P(2)—M(1)—N(1)		120.36	116.82
C(5)—C(6)	1.418	1.417	1.422	P(1)—M(1)—P(2)		119.27	126.36
C(6)—C(1)	1.461	1.458	1.464	O(1)—M(1)—P(1)	93.69	98.26	108.71
C(6)—N(1)	1.363	1.365	1.367	O(2)—M(1)—P(1)		91.43	86.79
C(12)—O(2)	1.322	1.309	1.314	O(1)—M(1)—P(2)		91.42	86.79
O(1)—M(1)	1.946	2.067	2.284	O(2)—M(1)—P(2)	102.49	98.26	108.63
N(1)—M(1)	2.055	2.016	2.275				
O(2)—M(1)	1.951	2.067	2.285				
P(1)—M(1)	2.638	2.451	2.699				
P(2)—M(1)		2.451	2.699				

Note. The C(1)—C(6)—C(7)—C(12) dihedral angles for complexes **4**, **5a**, and **5b** are 11.16°, 22.95°, and 31.87°, respectively.

lar structures of the complexes were calculated assuming no symmetry elements (C_1), the optimized geometric parameters suggest equivalence of two parts of the tridentate (O,N,O) ligands in complexes **4** and **5a**,**b** and a symmetric arrangement of two trimethylphosphine ligands in the coordination sphere of zinc and cadmium in complexes **5a**,**b**.

The phoshporus atom of the trimethylphosphine ligand in complex **4** (see Fig. 6, *a*) is near the plane of the paramagnetic (O,N,O) ligand, *i.e.*, the N(1)—Mg(1)—P(1) angle is 174.3°, which predetermines a low HFI constant of the unpaired electron with the magneic phosphorus nucleus. Conversely, the N(1)—M(1)—P(1) angle in the five-coordinate zinc and cadmium complexes is 120.4° for **5a** and 116.8° for **5b** (see Fig. 6, *b*). The M(1)—P(1) distance increases from 2.45 to 2.70 Å on going from zinc to cadmium, which also causes a significant decrease in the parameter $a_i(^{31}P)$ for complex **5b** compared to **5a**. According to DFT calculations, the molecular orbital occupied by the unpaired electron (HOMO) is predominantly localized on the (O,N,O) ligand (Fig. 7). The Mulliken spin density on the metal atom and phosphine ligands for complexes **4**, **5a**, and **5b** is at most 1%.

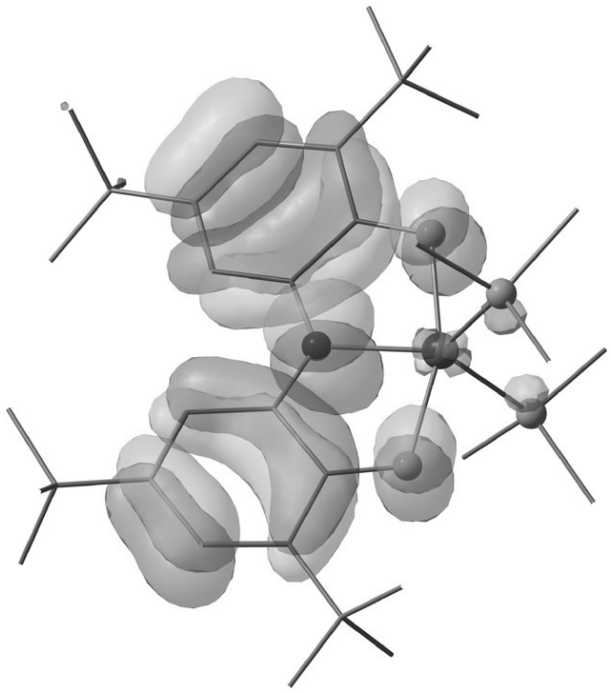

Fig. 7. View of the HOMO of complex **5a**.

The geometric characteristics of the tridentate (O,N,O) ligands for complexes **4**, **5a**,**b** are close to one another and match the criterion formulated in Ref. 16 for the dianion L^2, *viz.*, the so-called alternation parameter of the bond lengths in the six-membered ring C(1)—C(6) $\Delta a = C_{34} - (C_{23} + C_{45})/2$. It is 0.0300, 0.0290, and 0.0295 Å for **4**, **5a**, and **5b**, respectively, and in good agreement with the data of Refs 15 and 16. Despite the close values of the corresponding C—C, C—N, and C—O bond lengths in complexes **4**, **5a**,**b**, there is a significant difference in the geometry of the (O,N,O) ligand in these compounds. On going from magnesium to zinc and cadmium, the dihedral angle between the planes of the six-membered rings C(1)—C(6) and C(7)—C(12) increases considerably (see Table 3).

Experimental

Complexes **2a**—**f**, **4**, and **5a**—**c** were synthesized and studied under reduced pressure in the absence of oxygen and atmospheric moisture.

IR spectra were recorded on a FSM-1201 FT-IR spectrometer in Nujol in KBr cells. ESR spectra were recorded on a Bruker EMX spectrometer. Diphenylpicrylhydrazyl was used as a reference in the determination of the *g*-factor ($g = 2.0037$). Exact values of HFI constants were obtained by simulation of the spectra using the Win EPR Simfonia program. ^{1}H NMR spectra were obtained in $CDCl_3$ on a Bruker Avance III (400 MHz) spectrometer using Me_4Si as the internal standard.

The solvents used were purified and dried according to known procedures.[30] Complexes **1a**,**e**,**f**,[4] **1b**,[13] and bis(2-hydroxy-3,5-di-*tert*-butylphenyl)amine,[31] as well as the magnesium,[18] zinc,[19] and calcium[18] diazabutadiene complexes were prepared according to the published procedures.

Synthesis of complexes 1c,d (general procedure). To a solution of bis(2-hydroxy-3,5-di-*tert*-butylphenyl)amine (1 mmol) and a corresponding metal salt ($Sr(NO_3)_2 \cdot 4H_2O$ or $Ba(OAc)_2 \cdot 3H_2O$) (0.5 mmol) in methanol (20 mL), triethylamine (0.6 mL) was added. This was accompanied by strong blue-green coloration of the reaction mixture and by the formation of a dark precipitate. The precipitate of the complexes obtained was collected on a Schott glass filter No. 4.

Complex **1c**. The yield was 0.34 g (73%). Found (%): C, 72.16; H, 8.67; N, 2.92; Sr, 9.27. $C_{56}H_{80}N_2O_4Sr$. Calculated (%): C, 72.10; H, 8.64; N, 3.00; Sr, 9.39. IR, ν/cm^{-1}: 1639.7 m, 1612.2 m, 1549.6 s, 1529.8 m, 1360.5 s, 1348.3 m, 1322.3 w, 1291.8 s, 1259.8 s, 1203.3 s, 1180.4 w, 1162.1 m, 1119.4 w, 1099.6 s, 1085.9 m, 1035.5 m, 1023.3 s, 995.9 s, 933.3 m, 898.2 s, 861.6 s, 828.0 m, 803.6 m, 794.5 m, 733.5 m, 646.5 w, 620.5 m, 583.5 m, 524.4 m, 498.5 m. ^{1}H NMR (δ): 7.07 (d, 4 H, CH_{arom}, $J = 1.64$ Hz); 6.91 (d, 4 H, CH_{arom}, $J = 1.64$ Hz); 1.21 (s, 36 H, Bu^t); 1.11 (s, 36 H, Bu^t).

Complex **1d**. The yield was 0.30 g (62%). Found (%): C, 68.52; H, 8.26; N, 2.72; Ba, 13.90. $C_{56}H_{80}N_2O_4Ba$. Calculated (%): C, 68.45; H, 8.21; N, 2.85; Ba, 13.98. IR, ν/cm^{-1}: 1639.3 w, 1617.5 w, 1599.4 w, 1549.9 s, 1523.3 m, 1359.0 s, 1348.2 m, 1287.8 s, 1278.1 s, 1257.6 s, 1249.1 s, 1202.0 m, 1177.8 w, 1159.7 w, 1119.9 w, 1099.3 s, 1032.9 s, 1022.0 s, 993.0 s, 942.3 w, 930.2 w, 898.8 s, 865.0 s, 834.8 w, 825.1 w, 804.6 w, 794.9 m, 733.3 m, 724.9 m, 617.4 s, 582.3 w, 524.3 w, 497.8 w. ^{1}H NMR (δ): 7.08 (d, 4 H, CH_{arom}, $J = 1.84$ Hz); 6.85 (d, 4 H, CH_{arom}, $J = 1.84$ Hz); 1.22 (s, 36 H, Bu^t); 1.14 (s, 36 H, Bu^t).

Synthesis of complexes 2a—f (general procedure). Equimolar amounts of complexes **1a—f** and reducing agents were mixed in an ESR tube in the corresponding solvent (see Scheme 2). The formation of complexes **2a**,**b**,**e** proceeds at the rate of reactant mixing. The reactions with metals (preparation of compounds **2c**,**d**,**f**) were conducted until complete dissolution of the metals. Complexes **2a—f** were studied in solution without isolation. The concentration of paramagnetic species in the solutions of compounds **2a—f** was in the range from $5 \cdot 10^{-4}$ to $1 \cdot 10^{-3}$ mol L^{-1}.

Synthesis of complex 3. A solution of complex **2d** in 1,2-dimethoxyethane was kept at room temperature for 1 month. Complex **3** was isolated from the reaction mixture as a fine-crystalline dark-green substance. The yield was 0.12 g (42%). Found (%): C, 66.17; H, 8.72; N, 2.38; Ba, 11.76. $C_{64}H_{100}N_2O_8Ba$. Calculated (%): C, 66.11; H, 8.67; N, 2.41; Ba, 11.81. IR, ν/cm^{-1}: 1639.7 w, 1619.2 w, 1602.4 w, 1550.0 s, 1523.6 m, 1360.4 s, 1349.7 m, 1283.6 s, 1279.8 s, 1256.2 s, 1250.6 s, 1246.1 m, 1202.9 m, 1179.2 w, 1122.3 w, 1089.7 s, 1030.2 s, 1026.0 s, 997.0 s, 947.6 w, 932.7 w, 889.9 s, 872.2 s, 835.0 w, 827.4 w, 804.8 w, 797.7 m, 736.1 m, 727.1 m, 616.2 s, 581.4 w. ^{1}H NMR (δ): 7.08 (d, 4 H, CH_{arom}, $J = 1.80$ Hz); 6.93 (d, 4 H, CH_{arom}, $J = 1.80$ Hz); 3.56 (s, 8 H, CH_2); 3.39 (s, 12 H, CH_3); 1.21 (s, 36 H, Bu^t); 1.18 (s, 36 H, Bu^t).

Synthesis of complexes 4, 5a,b (general procedure). An excess amount of trialkylphosphine was condensed into an ESR tube containing frozen solutions of compounds **2a**,**e**,**f** in THF. Complexes **4**, **5a**,**b** were studied in solution without isolation. The concentration of paramagnetic species in the solutions of compounds **4**, **5a**,**b** was in the range $1 \cdot 10^{-3}$—$1 \cdot 10^{-2}$ mol L^{-1}.

X-ray diffraction analysis. An X-ray diffraction study of complex **3** was performed on a Smart Apex diffractometer (Mo-Kα-radiation, graphite monochromator). The structure was solved by the direct method and refined by the full-matrix least-squares method over F^2 by the SHELXTL program (see Ref. 32). The absorption correction was applied using the SADABS program (see Ref. 33). All non-hydrogen atoms were refined in the anisotropic approximation. The hydrogen atoms in the structure of complex **3** were placed in the geometrically calculated positions and refined in the riding model. The crystal size was 0.22×0.10×0.08 mm. A total of 81292 reflections were measured, among which 27002 ($R_{int} = 0.0532$) were independent with $I > 2\sigma(I)$. The unit cell parameters for $C_{64}H_{99}BaN_2O_8$ at 150(2) K were as follows: $a = 18.0876(7)$ Å, $b = 18.5097(7)$ Å, $c = 39.2880(15)$ Å, $\beta = 97.2430(10)°$, monoclinic crystal system, space group $P2/n$, $Z = 8$, $V = 13048.5(9)$ Å^3, $d_{calc} = 1.183$ g cm^{-3}, $\mu = 0.659$ mm^{-1}, $F(000) = 4936$, $1.92° \le \theta \le 26.50°$, $R_1 = 0.0521$ and $wR_2 = 0.1145$ ($I > 2\sigma(I)$), $R_1 = 0.0941$ and $wR_2 = 0.1264$ (over all data)), $S(F^2) = 1.025$, the minimum and maximum residual electron densities were −0.544 and 1.13 e Å^{-3}, respectively.

Quantum chemical calculations. The geometries of complexes **4** and **5a,b** were optimized using the GAUSSIAN 03 program (see Ref. 34) and the B3LYP functional in the 6-31G* basis set for **4** and **5a** and DGDZVP basis set for **5b**. The absence of imaginary frequencies evidences that the equilibrium structures corresponds to the potential energy minima.

This work was financially supported by the Russian Foundation for Basic Research (Project Nos 10-03-00788-a, 11-03-97041-r_povolzh´e_a, and 11-03-97051-r_povolzh´e_a), the Council on Grants at the President of the Russian Federation (Programs NSh-7065.2010.3 and MK-641.2011.3), and the Ministry of Education and Science of the Russian Federation (Federal Target Program "Academic and Teaching Staff of the Innovative Russia" for 2009—2013, State contract P839 dated by 25.05.2010).

References

1. H. B. Stegman, K. Scheffler, F. Stocker, *Angew. Chem.*, *Int. Ed.*, 1970, **9**, 456.
2. H. B. Stegman, K. Scheffler, *Chem. Ber.*, 1970, **103**, 1279.
3. H. B. Stegman, K. Scheffler, F. Stocker, *Angew. Chem.*, *Int. Ed.*, 1971, **10**, 499.
4. A. I. Girgis, A. L. Balch, *Inorg. Chem.*, 1975, **14**, 2724.
5. S. K. Larsen, C. G. Pierpont, *J. Am. Chem. Soc.*, 1988, **110**, 1827.
6. C. L. Simpson, S. R. Boone, C. G. Pierpont, *Inorg. Chem.*, 1989, **28**, 4379.
7. S. Bruni, A. Ganeschi, F. Cariati, C. Delfs, D. Gatteschi, *J. Am. Chem. Soc.*, 1994, **118**, 1388.

8. B. R. McGarvey, A. Ozarowski, Zh. Tian, D. G. Tuck, *Can. J. Chem.*, 1995, **73**, 1213.
9. G. Speier, J. Csihony, A. M. Whalen, C. G. Pierpont, *Inorg. Chem.*, 1996, **35**, 3519.
10. S. N. Lyubchenko, V. A. Kogan, L. P. Olekhnovich, *Koord. Khim.*, 1996, **22**, 569 [*Russ. J. Coord. Chem.* (*Engl. Transl.*), 1996, **22**].
11. C. Camacho-Camacho, H. Tlahuext, H. Nöth, R. Contreras, *Heteroatom Chem.*, 1998, **9**, 321.
12. A. Bencini, I. Ciofini, E. Giannasi, C. A. Daul, K. Doclo, *Inorg. Chem.*, 1998, **37**, 3719.
13. C. Camacho-Camacho, G. Merino, F. J. Martinez-Martinez, H. Nöth, R. Contreras, *Eur. J. Inorg. Chem.*, 1999, 1021.
14. M. A. Brown, J. A. Castro, B. R. McGarvey, D. G. Tuck, *Can. J. Chem.*, 1999, **77**, 502.
15. P. Chaudhuri, M. Hess, K. Hildenbrand, E. Bill, T. Weyhermüller, K. Wieghardt, *Inorg. Chem.*, 1999, **38**, 2781.
16. A. G. Starikov, V. I. Minkin, R. M. Minyaev, V. V. Koval, *J. Phys. Chem. A*, 2010, **114**, 7780.
17. P. Clopath, A. V. Zelewsky, *Chem. Commun.*, 1971, 47.
18. P. Clopath, A. V. Zelewsky, *Helv. Chim. Acta*, 1972, **55**, 52.
19. G. A. Abakumov, V. K. Cherkasov, A. V. Piskunov, O. Yu. Trofimova, G. V. Romanenko, *Dokl. Akad. Nauk*, 2010, **434**, 344 [*Dokl. Chem.* (*Engl. Transl.*), 2010, **434**, 237].
20. J. Emsley, *The Elements*, Clarendon press, Oxford, 1991, 251 pp..
21. H. B. Stegmann, W. Uber, K. Scheffler, *Z. Anal. Chem.*, 1977, **286**, 59.
22. A. V. Piskunov, O. Yu. Sukhoshkina, I. V. Smolyaninov, *Zh. Obsch. Khim.*, 2010, **80**, 629 [*Russ. J. Gen. Chem.* (*Engl. Transl.*), 2010, **80**, 790].
23. A. I. Poddels´ky, V. K. Cherkasov, M. P. Bubnov, L. G. Abakumova, G. A. Abakumov, *J. Organomet. Chem.*, 2005, **690**, 145.
24. A. V. Piskunov, A. V. Maleeva, G. A. Abakumov, V. K. Cherkasov, G. K. Fukin, A. S. Bogomyakov, *Koord. Khim.*, 2011, **37**, 243 [*Russ. J. Coord. Chem.* (*Engl. Transl.*), 2011, **37**, 243].
25. G. A. Abakumov, V. K. Cherkasov, *Metalloorg. Khim.*, 1990, **3**, 838 [*Organomet. Chem. USSR* (*Engl. Transl.*), 1990, **3**, 426].
26. K. A. Kozhanov, M. P. Bubnov, V. K. Cherkasov, G. K. Fukin, G. A. Abakumov, *J. Chem. Soc., Dalton Trans.*, 2004, 2957.
27. G. A. Abakumov, A. V. Krashilina, V. K. Cherkasov, L. N. Zakharov, *Dokl. Akad. Nauk*, 2003, **391**, 343 [*Dokl. Chem.* (*Engl. Transl.*), 2003, **391**, 185].
28. S. Vongtragool, B. Gorshunov, M. Dressel, J. Krzystek, D. M. Eichhorn, J. Telser, *Inorg. Chem.*, 2003, **42**, 1788.
29. A. F. Cameron, K. P. Forrest, G. Ferguson, *J. Chem. Soc. A*, 1971, 1286.
30. A. J. Gordon, R. A. Ford, *The Chemist´s Companion*, Wiley Intersci. Publ., New York, 1972, 537 pp.
31. A. I. Poddel´sky, N. N. Vavilina, N. V. Somov, V. K. Cherkasov, G. A. Abakumov, *J. Organomet. Chem.*, 2009, **694**, 3462.
32. G. M. Sheldrick, *SHELXTL v. 6.12, Structure Determination Software Suite*, Bruker AXS, Madison (WI), USA.
33. G. M. Sheldrick, *SADABS v.2.01, Bruker/Siemens Area Detector Absorption Correction Program*, Bruker AXS, Madison (WI), USA.
34. M. J. Frisch, G. W. Trucks, H. B. Schlegel, M. J. Frisch, G. W. Trucks, H. B. Schlegel, G. E. Scuseria, M. A. Rob, J. R. Cheeseman, J. A. Montgomery, Jr., T. Vreven, K. N. Kudin, J. C. Burant, J. M. Millam, S. S. Iyengar, J. Tomasi, V. Barone, B. Mennucci, M. Cossi, G. Scalmani, N. Rega, G. A. Petersson, H. Nakatsuji, M. Hada, M. Ehara, K. Toyota, R. Fukuda, J. Hasegawa, M. Ishida, T. Nakajima, Y. Honda, O. Kitao, H. Nakai, M. Klene, X. Li, J. E. Knox, H. P. Hratchian, J. B. Cross, V. Bakken, C. Adamo, J. Jaramillo, R. Gomperts, R. E. Stratmann, O. Yazyev, A. J. Austin, R. Cammi, C. Pomelli, J. W. Ochterski, P. Y. Ayala, K. Morokuma, G. A. Voth, P. Salvador, J. J. Dannenberg, V. G. Zakrzewski, S. Dapprich, A. D. Daniels, M. C. Strain, O. Farkas, D. K. Malick, A. D. Rabuck, K. Raghavachari, J. B. Foresman, J. V. Ortiz, Q. Cui, A. G. Baboul, S. Clifford, J. Cioslowski, B. B. Stefanov, G. Liu, A. Liashenko, P. Piskorz, I. Komaromi, R. L. Martin, D. J. Fox, T. Keith, M. A. Al-Laham, C. Y. Peng, A. Nanayakkara, M. Challacombe, P. M. W. Gill, B. Johnson, W. Chen, M. W. Wong, C. Gonzalez, J. A. Pople, *Gaussian 03, Revision A.1*, Gaussian, Inc., Pittsburgh (PA), 2003.

Received July 18, 2011;
in revised form October 10, 2011